Electronic Supplementary Information

Wood-based electrolyte with reversible phase transition for smart thermal shutdown self-protection

Qingtao Zeng, Xuejun Lai*, Hongqiang Li, Zhonghua Chen, Xingrong Zeng, Liqun Zhang*

School of Materials Science and Engineering, Key Lab of Guangdong Province for High Property and Functional Polymer Materials, South China University of Technology, No 381, Wushan Road, Tianhe District, Guangzhou 510640, China

---

*Corresponding Authors:

Prof. Xuejun Lai, E-mail: msxjlai@scut.edu.cn; Prof. Liqun Zhang, E-mail: liqunzhang@scut.edu.cn

Table S1. Formula of SPEs.

Sample	PEO-PPO-PEO (g)	H_2O (g)	LiCl (g)	LiCl concentration (mol/L)
SPE-0	1.5	3.5	0	0
SPE-1	1.5	3.5	0.105	0.5
SPE-2	1.5	3.5	0.210	1.0
SPE-3	1.5	3.5	0.315	1.5
SPE-4	1.5	3.5	0.420	2.0

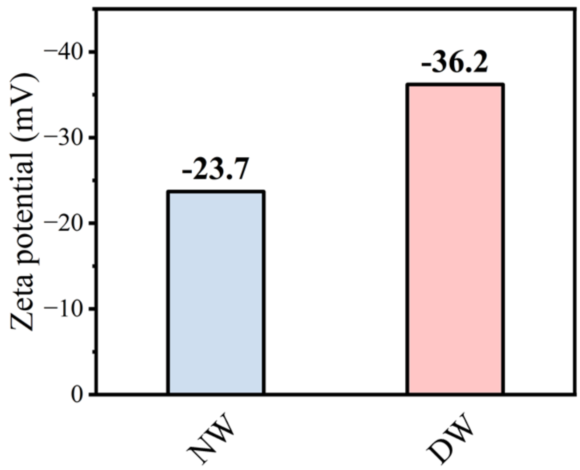

Figure S1. Zeta potential of NW and DW.

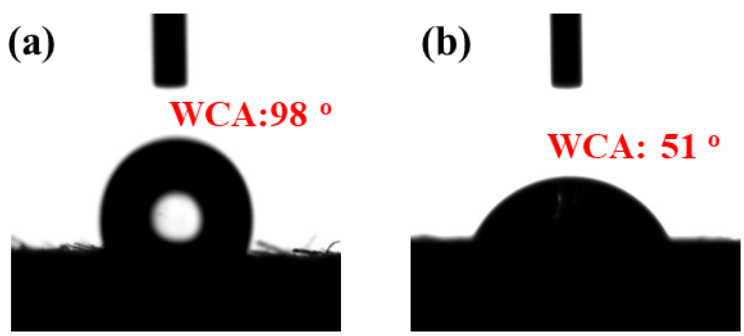

Figure S2. WCA of (a) NW and (b) DW.

Table S2. Physical properties of NW and DW.

Sample	Density ($mg \cdot cm^{-3}$)	Specific surface area ($m^2 \cdot g^{-1}$)
NW	101±3	1.7±0.4
DW	83±5	9.1±1.3

Table S3. Absorption capacity of SPE solution in DW.

Sample	Absorption capacity ($g \cdot g^{-1}$)
SPE-0	10.59±0.28
SPE-1	11.46±0.37
SPE-2	10.92±0.20
SPE-3	10.73±0.32
SPE-4	11.20±0.25

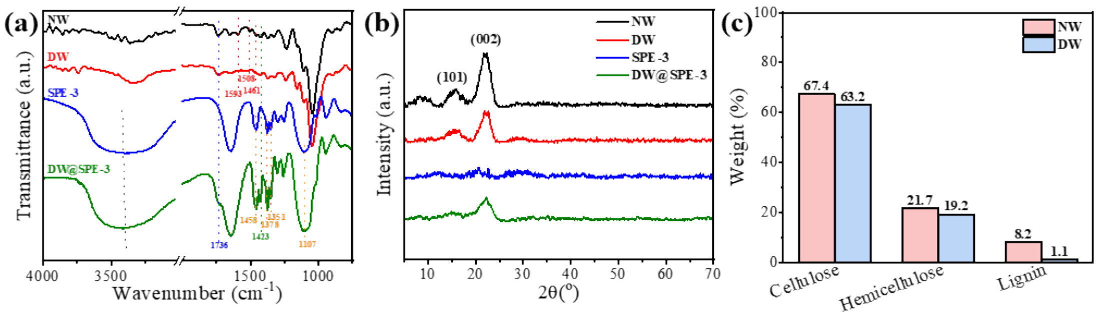

Figure S3. (a) FTIR and (b) XRD spectra of NW, DW, SPE-3 and DW@SPE-3. (c) Content of cellulose, hemicellulose and lignin of NW and DW.

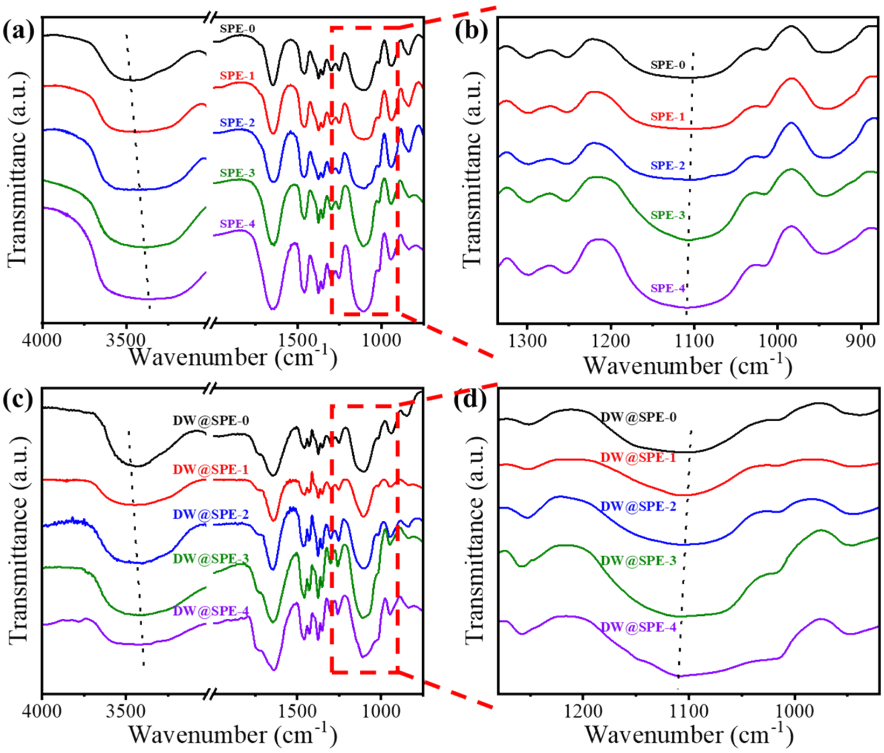

Figure S4. FTIR spectra of (a, b) SPEs and (c, d) DW@SPEs.

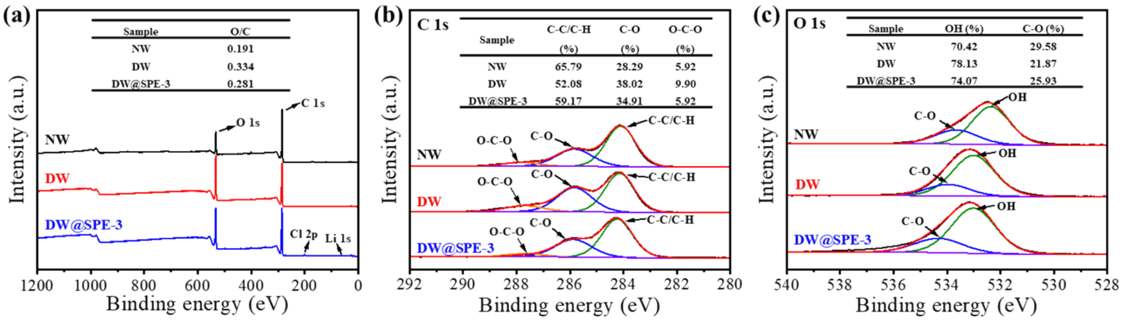

Figure S5. (a) XPS, (b) C 1s XPS and (c) O 1s XPS spectra of NW, DW and DW@SPE-3

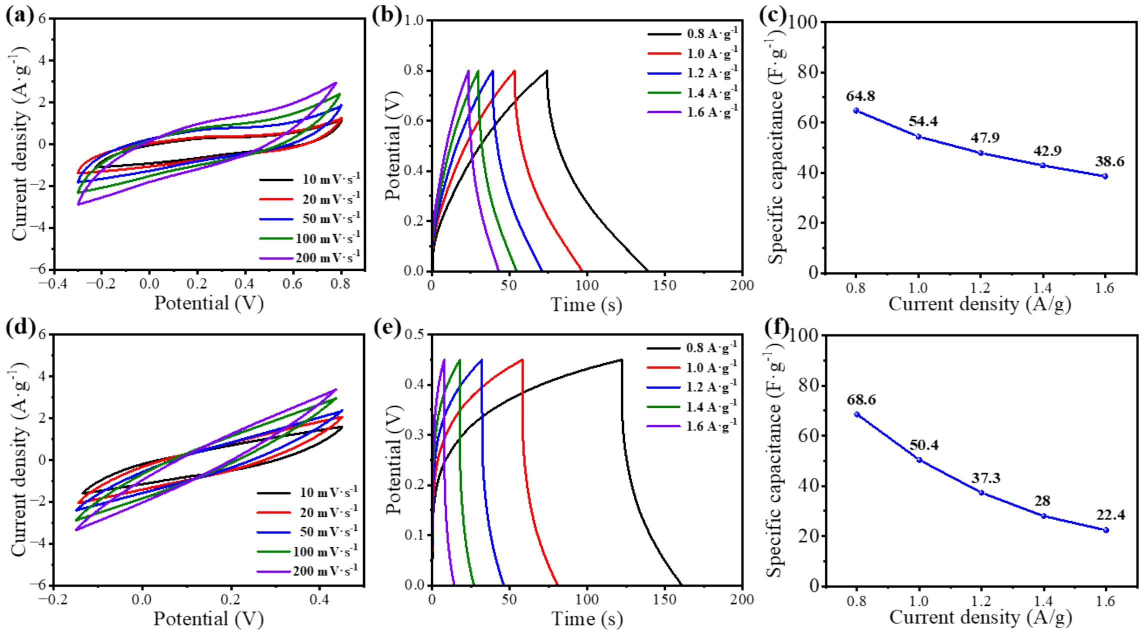

Figure S6. (a, d) CV curves, (b, e) GCD curves and (c, f) specific capacitance of SPE-3 aqueous solution and DW@SPE-3 in the R direction (a-c: SPE-3 aqueous solution, and d-f: DW@SPE-3 in the R direction).

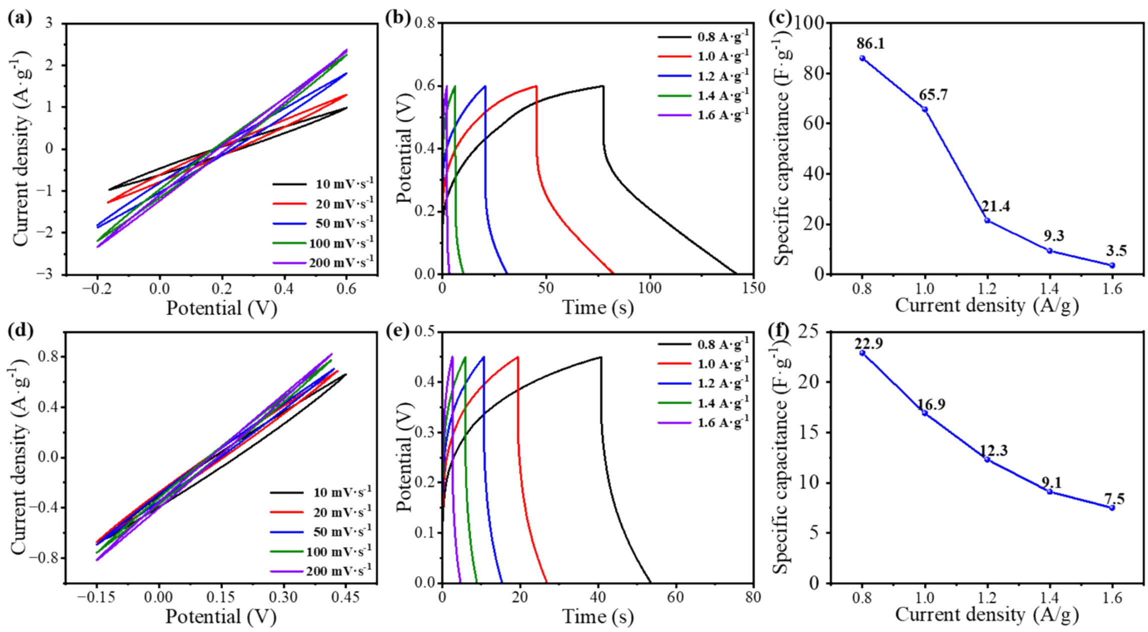

Figure S7. (a, d) CV curves, (b, e) GCD curves and (c, f) specific capacitance of NW@SPE-3 (a-c: in the L direction, and d-f: in the R direction).

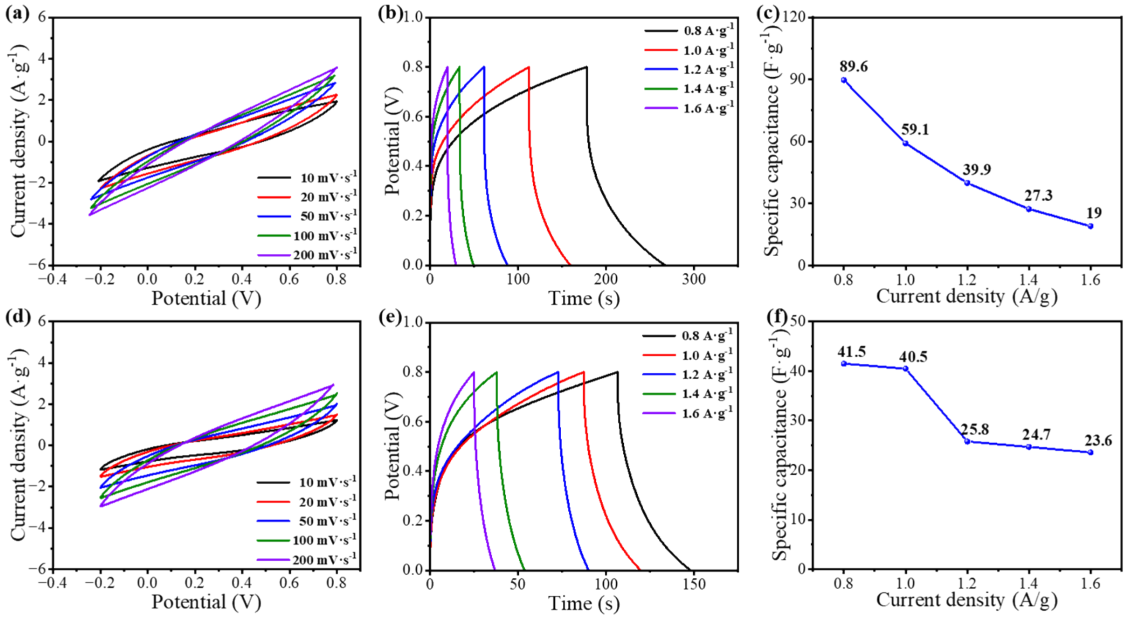

Figure S8. (a, d) CV curves, (b, e) GCD curves and (c, f) specific capacitance (a-c: PU@SPE-3, and d-f: BC@SPE-3).

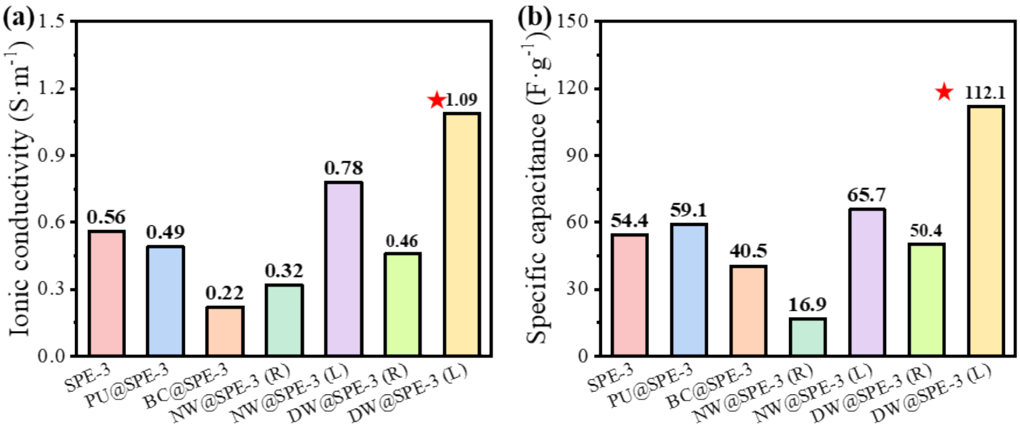

Figure S9. (a) Ionic conductivity and (b) specific capacitance (1.0 A·g^{-1}) of SPE-3, PU@SPE-3, BC@SPE-3, NW@SPE-3 and DW@SPE-3 (in the L direction).

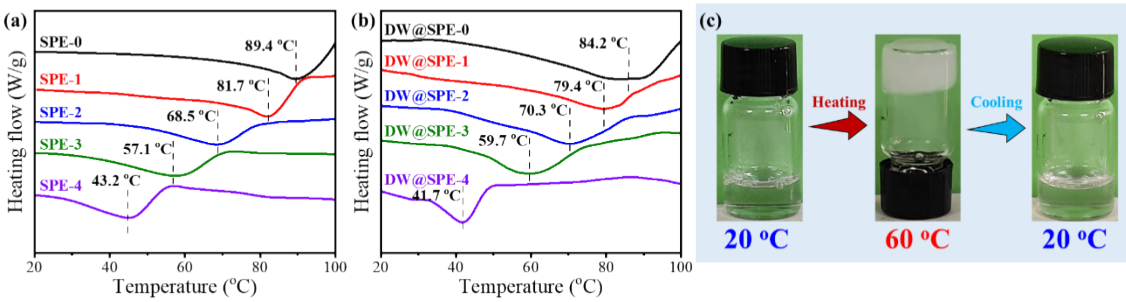

Figure S10. DSC curves of (a) SPEs and (b) DW@SPEs. (c) Sol-gel phase transition of SPE-3.

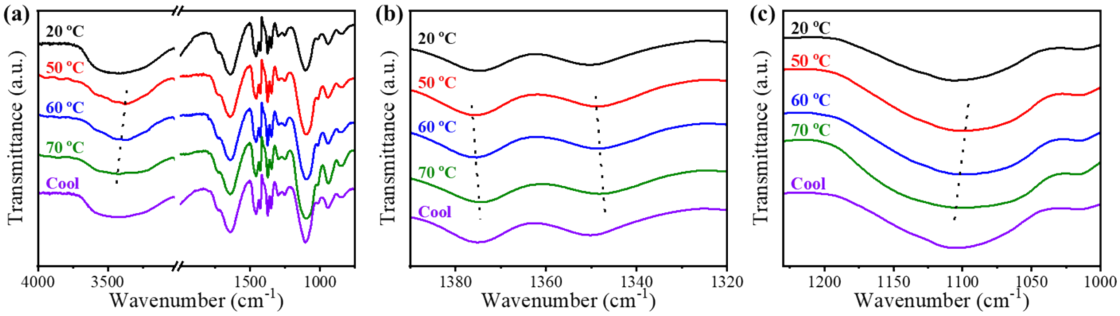

Figure S11. FTIR spectra of DW@SPE-3 at different temperatures.

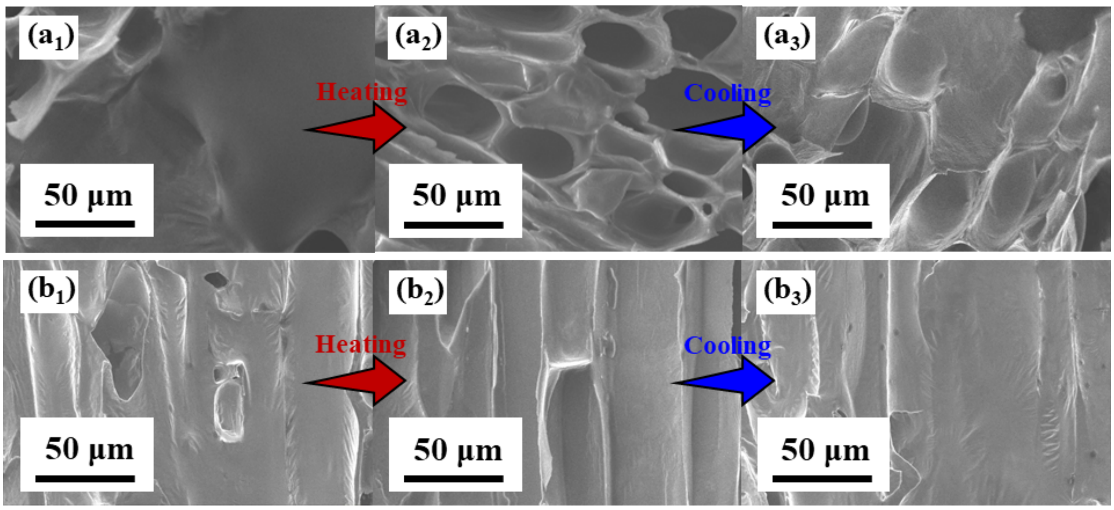

Figure S12. SEM image of DW@SPE-3: (a_1, b_1) 20 °C, (a_2, b_2) 60 °C and (a_3, b_3) after cooling down to 20 °C.

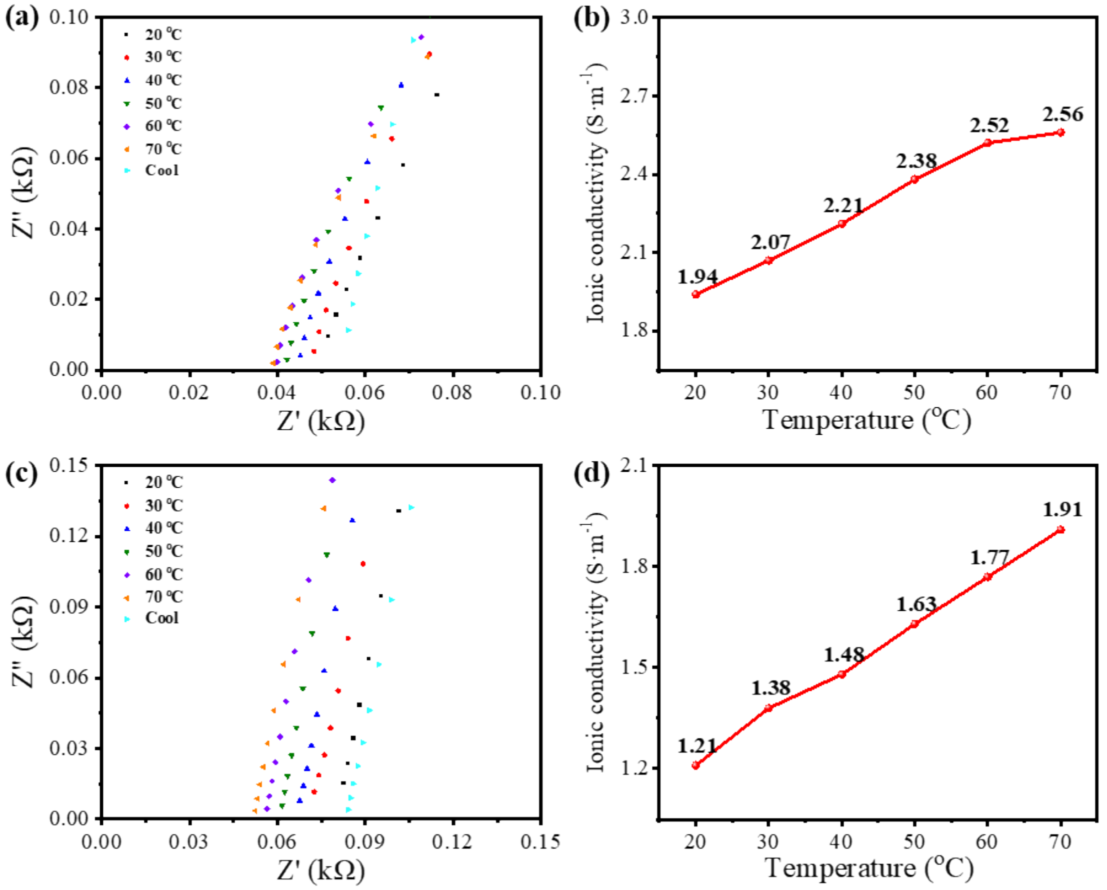

Figure S13. (a, c) EIS plots and (b, d) ionic conductivity of DW@LiCl at different temperatures (a and b: in L direction, and c and d: in R direction.)

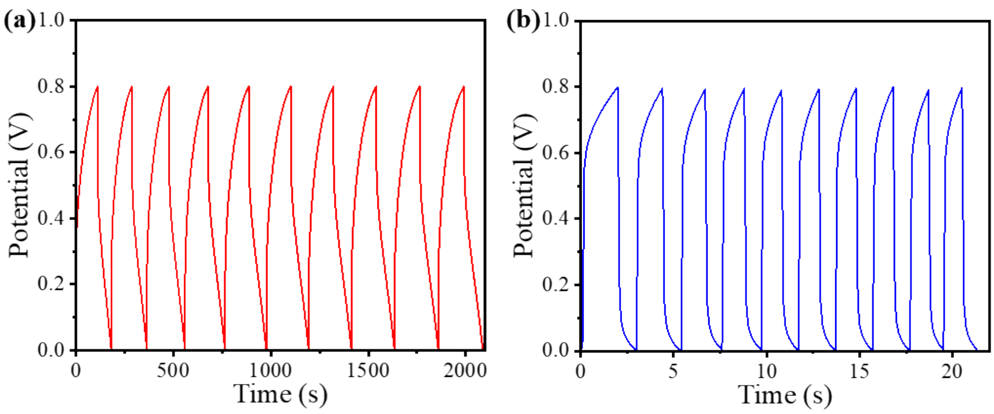

Figure S14. Cyclic GCD curves of DW@SPE-3 at (a) 20 and (b) 70 °C (1.0 $A \cdot g^{-1}$).

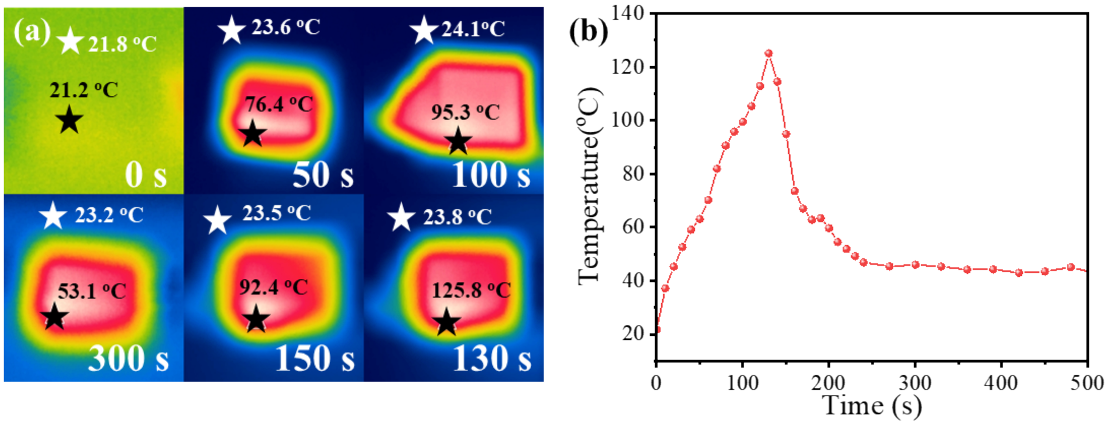

Figure S15. (a) Infrared thermal images and (b) real-time temperature-time curve of electrothermal self-protection test of DW@LiCl in L direction.

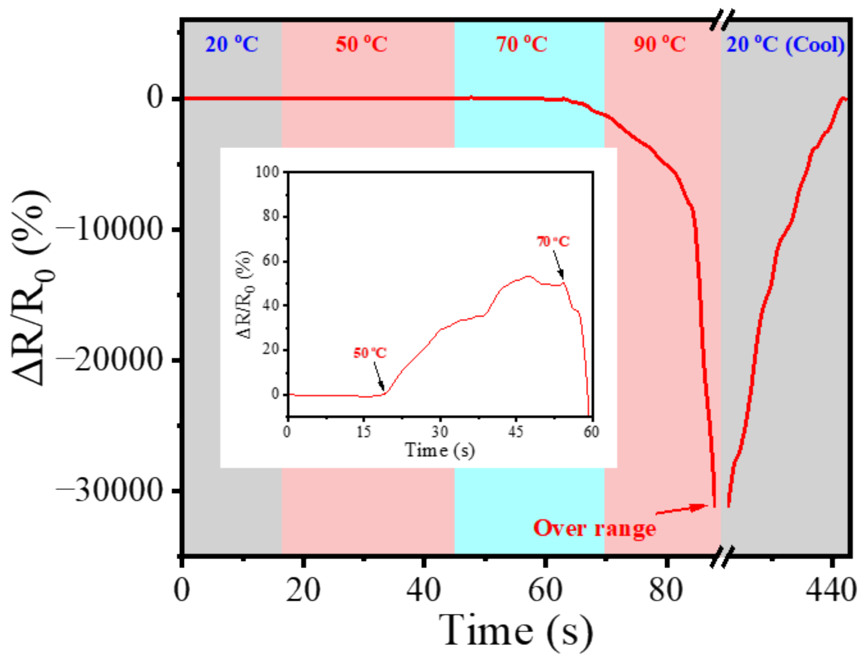

Figure S16. Real-time $\Delta R/R_0$-time curve of DW@SPE-3 in L direction.

Table S4. Comparison of temperature-sensing performance between DW@SPE and other materials.

Materials	Maximum TCR (%·$^{o}C^{-1}$)	Temperature range (^{o}C)	Ref
Pt/silk fibroin	-0.21	20-220	S1
PVA/CA/AgNP	-0.08	30-40	S2
TPU and PEDOT:PSS	-0.04	25-100	S3
PSS-CNT&CS/CF	-0.47	30-100	S4
CNF-MXene-Fe_3O_4 and PAAm	-0.17	40-100	S5
RGO/PU	-0.36	20-90	S6
DW@SPE-3	-0.54	20-200	This work

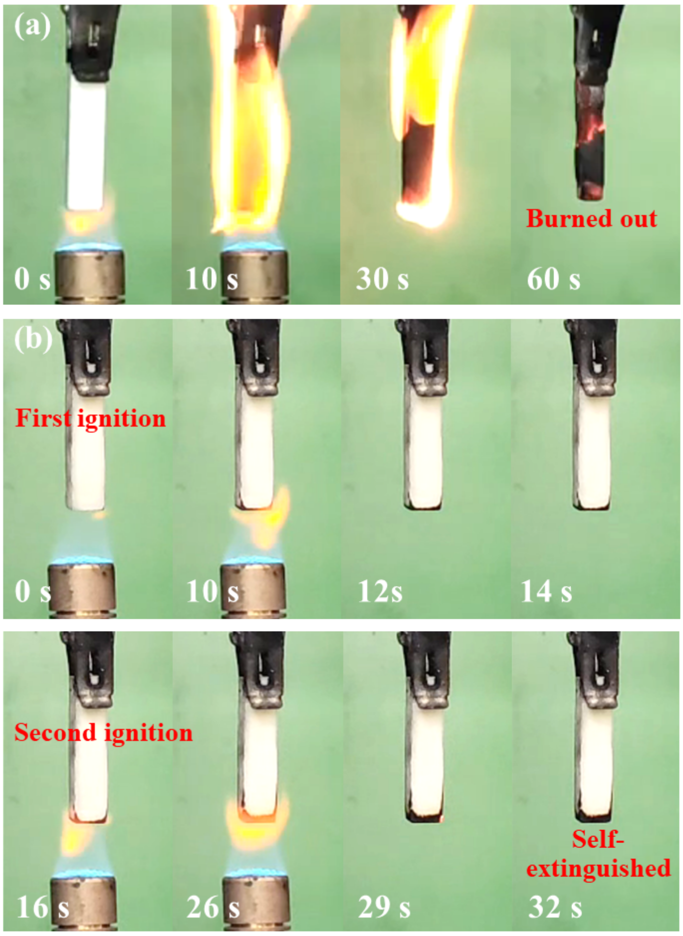

Figure S17. Video snapshots of vertical burning test of (a) DW@SPE-0 and (b) DW@SPE-3 after being placed in 60 °C vacuum oven for 12 h.

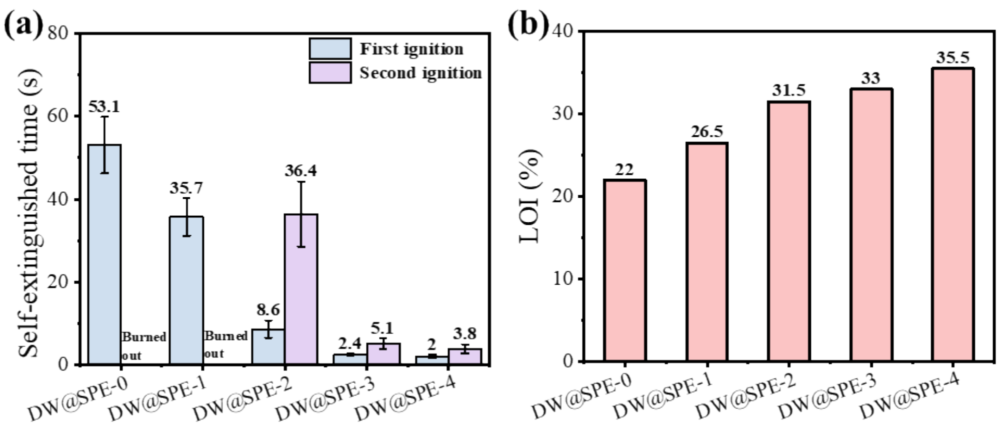

Figure S18. (a) Self-extinguished time in vertical burning test and (b) LOI value of DW@SPEs after being placed in 60 °C vacuum oven for 12 h.

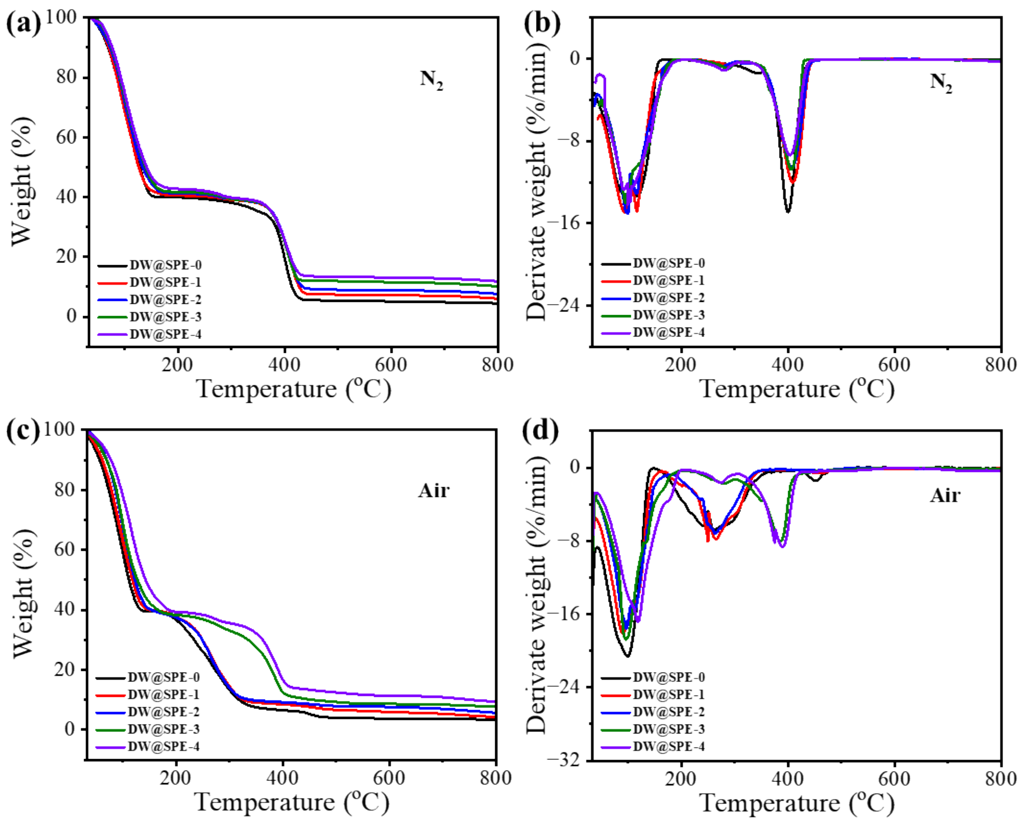

Figure S19. (a, c) TGA and (b, d) DTG curves of DW@SPEs under N_2 and air atmosphere.

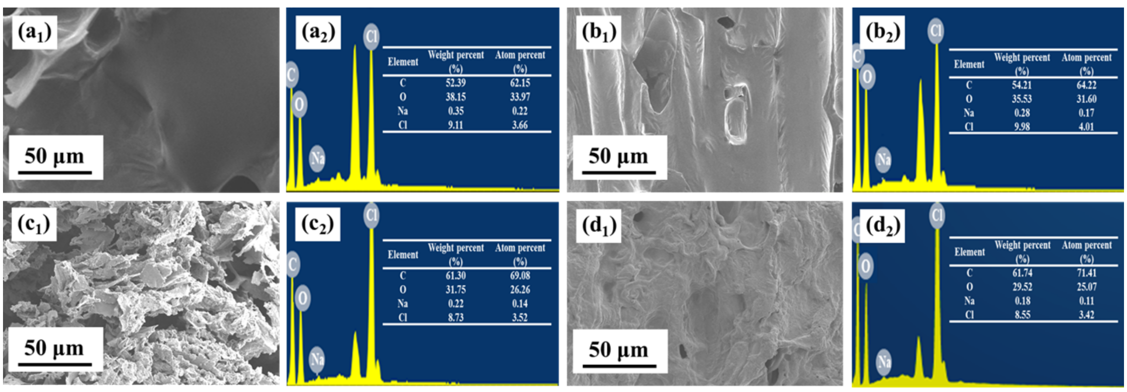

Figure S20. SEM-EDX images of DW@SPE-3 (a, b) before and (c, d) after burning (a and c: in the L direction, and b and d: in the R direction).

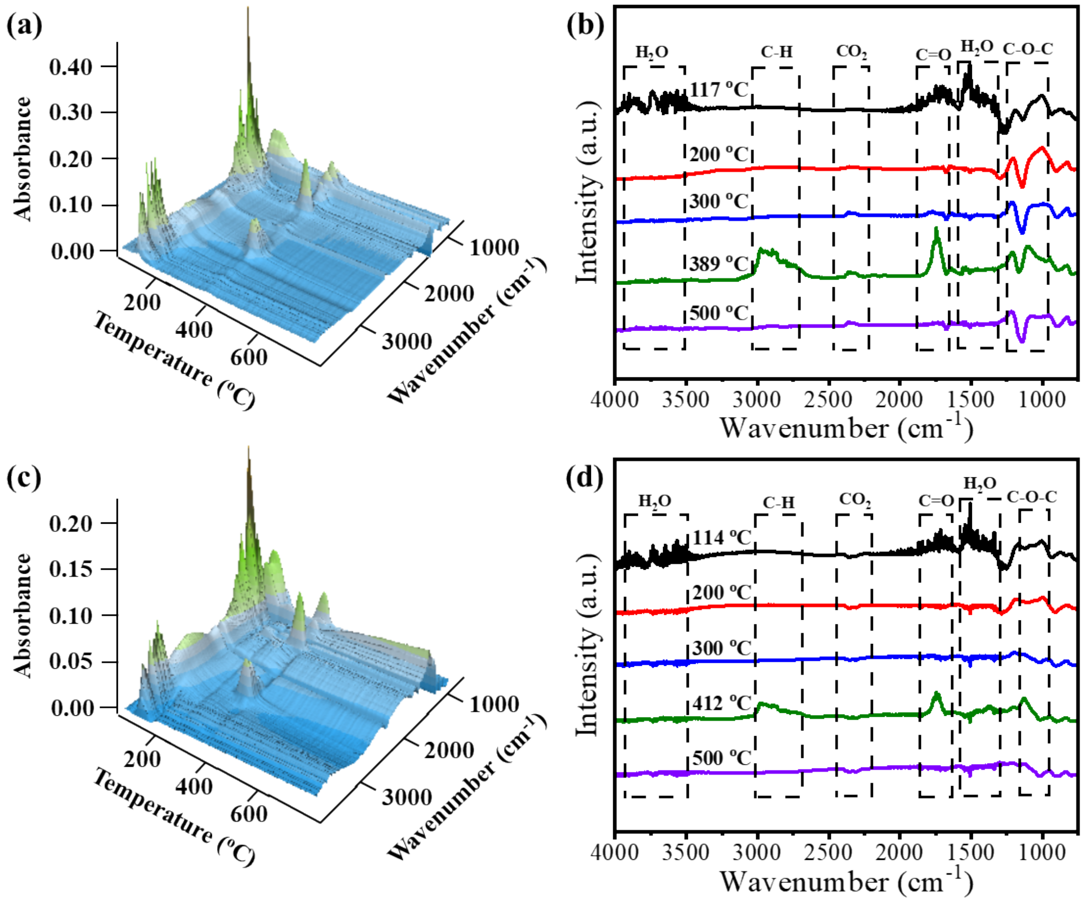

Figure S21. 3D TG-FTIR and the corresponding FTIR spectra of (a, b) DW@SPE-0 and (c, d) DW@SPE-3.

References

[S1] J. Huang, Z. Xu, W. Qiu, F. Chen, Z. Meng, C. Hou, W. Guo and X. Liu, *Adv. Funct. Mater.*, 2020, **30**, 1910547.

[S2] L. Chen, X. Chang, H. Wang, J. Chen and Y. Zhu, *Nano Energy*, 2022, **96**, 107077.

[S3] P. Wang, W. Yu, G. Li, C. Meng and S. Guo, *Chem. Eng. J.*, 2023, **452**, 139174.

[S4] Y. Zhang, Y. Li, A. Du, Y. Wu and J. Zeng, *J. Mater. Sci. Technol.*, 2024, **173**, 114-120.

[S5] Y. He, Y. Wei, Y. Qian, C. Wang, Y. Liu, Z. Ye and G. Chen, *J. Mater. Chem. A*, 2022, **10**, 18856-18865.

[S6] W. Xiao, L. Wang, B. Li, Y. Li, Y. Wang, J. Luo, X. Huang, A. Xie and J. Gao, *J. Colloid. Interf. Sci.*, 2022, **608**, 931-941.